Chirality

DOI: 10.1002/ange.200904979

2D Random Organization of Racemic Amino Acid Monolayers Driven by Nanoscale Adsorption Footprints: Proline on Cu(110)**

*Matthew Forster, Matthew S. Dyer, Mats Persson, and Rasmita Raval**

The way in which chiral molecules interact, aggregate, and organize has attracted intense investigation since the discovery of molecular chirality by Pasteur.[1] Upon association, enantiomers may yield a racemic compound, spontaneously separate to form a conglomerate, or congregate as a random solid solution.[2] The outcome is of central importance in chiral science and technology since it governs the physical, chemical, and biological function of the system. However, a detailed understanding of the underlying driving forces remains to be gained.[3] Recently, the organization of chiral molecules adsorbed at surfaces has provided a unique opportunity to witness the nanoscale details of molecules interacting in 2D, using scanning tunneling microscopy (STM).[4] Of particular interest is the organization of amino acids at surfaces,[5–12] which represent important interfaces in sensors,[13] enantioselective catalysis,[14] and molecular electronics.[15] The behavior of racemic mixtures of amino acids is also highly pertinent to the chiral separations industry[2,16] and has implications in the origin of homochirality of life,[17] with surfaces providing potential asymmetrizing environments for racemic prebiotic mixtures. Although the behavior of enantiopure amino acids at surfaces is beginning to be captured,[5–11] detailed characterization has remained elusive since it requires information on the conformation of individual adsorbed molecules, their bonding points with the surface, and the resultant molecular adsorption footprint.[9,18] This difficulty is greatly compounded when considering a racemic system in which information needs to be tracked for each enantiomer. Recently, we have characterized enantiopure (*S*)-proline on Cu(110) (Figure 1a) at the single-molecule level,[12] ascertaining the individual conformations and adsorption footprints. This system, therefore, gives a unique opportunity to study and unravel the behavior of the racemic system.

Herein, we present the first molecule-by-molecule mapping of a racemic amino acid system at a surface, showing the structure of the (4×2) monolayer of (*R*,*S*)-proline on Cu(110) is driven, not by molecular chirality, but by the chirality of the adsorption footprint. This situation leads to a random arrangement of molecular chirality but results in a strict heterochiral adsorption-footprint pattern. This effectively creates a 2D random solid solution, which is a rare occurrence in 3D crystals[2] but, interestingly, may become more prevalent in 2D owing to surface interactions, as shown herein. For amino acids, this behavior is a departure from that found in 3D where they crystallize as racemic compounds.[19] Our work provides an important advance into understanding amino acid ordering at surfaces, with insights provided by STM, low-energy electron diffraction (LEED), reflection absorption infrared spectroscopy (RAIRS), and periodic density-functional theory (DFT).

Enantiopure (*S*)-proline on Cu(110) creates an organized (4×2) overlayer (Figure 1a), containing two distinct prolate conformers, which are a consequence of the three-point bonding interaction of the molecule with the surface,[12] in which the two carboxylate oxygen atoms bind to adjacent copper atoms in the $[1\bar{1}0]$ row, with the third bonding contact being through the nitrogen atom to a copper atom directly opposite in the neighboring row. If the nitrogen bonds to the copper atom to the left, a left-handed triangular adsorption footprint is described and the pyrrolidine ring tilts significantly away from the surface (conformer A, Figure 1b), imaging as a bright protrusion in STM. If the nitrogen bonds to the right, a right-handed triangular adsorption footprint is described, the ring lies flat (conformer B, Figure 1b) and images as a faint protrusion. Therefore, the adsorption footprints adopted within the (4×2) organization are experimentally distinguishable at the single-molecule level. The left- and right-handed triangular adsorption footprints generate chiral mirror images in two-dimensions.[18] Thus, the enantiopure (4×2) overlayer has a heterochiral footprint arrangement (Figure 1c).

Comparing the STM images from enantiopure (*S*)- and (*R*)-proline enables the molecular chirality to be distinguished (Figure 1d) with the A conformers of (*S*)- and (*R*)-proline imaging as bright ovals (at high image contrast) slanted in mirror directions with respect to the $[1\bar{1}0]$ axis, and the B conformers of (*S*)- and (*R*)-proline imaging as fainter but distinct triangles, also slanted in mirror directions. Thus,

[*] M. Forster, Dr. M. S. Dyer, Prof. R. Raval
Surface Science Research Centre and Department of Chemistry, University of Liverpool
Liverpool, L69 3BX (UK)
E-mail: r.raval@liv.ac.uk
Prof. M. Persson
Surface Science Research Centre and Department of Chemistry, University of Liverpool
Liverpool, L69 3BX (UK)
and
Department of Applied Physics, Chalmers University of Technology
41296 Göteborg (Sweden)

[**] R.R. and M.F. acknowledge the EPSRC, NERC, EU 7th framework small scale collaborative project RESOLVE (NMP4-SL-2008-214340), and the University of Liverpool for equipment grants, funding and a studentship for M.F. M.P acknowledges the Swedish Research Council (VR) and the Marie Curie Research Training Network PRAIRIES, contract MRTN-CT-2006-035810. M.S.D. acknowledges the University of Liverpool for funding of a post-doctoral fellowship and computational resources.

Supporting information for this article is available on the WWW under http://dx.doi.org/10.1002/anie.200904979.

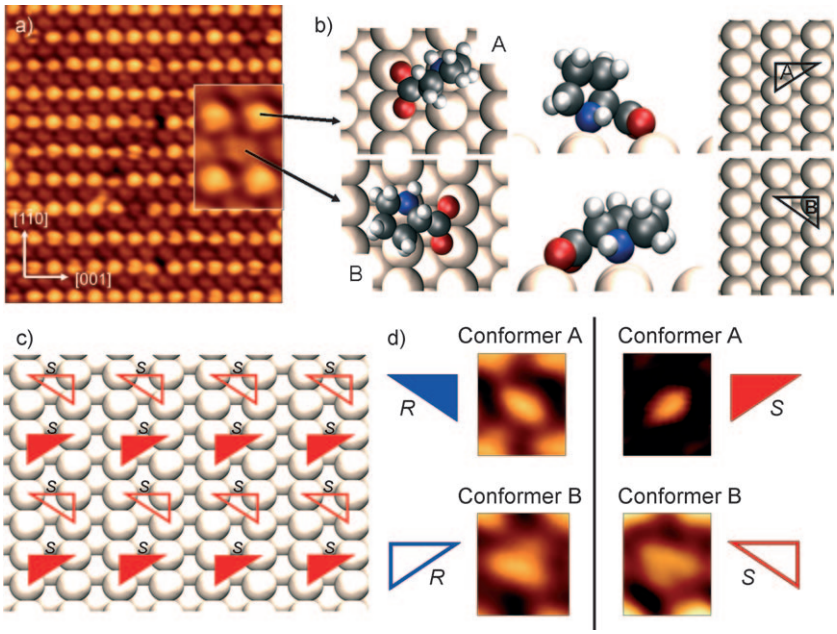

Figure 1. a) STM image of the (4×2) overlayer of (*S*)-proline on Cu(110) (94×102 Å^2, $I(t) = -0.4$ nA, $V(t) = -806$ mV). Inset: Enlarged STM image of a (4×2) unit showing conformers A (bright) and B (faint), arrows point to relaxed adsorption geometries for conformers A and B shown in b) from left to right: view from above, the side, and in terms of their triangular adsorption footprint (red O, blue N, black C, and white H). c) Schematic diagram showing the preferred adsorption-footprint arrangement of the enantiopure (*S*)-proline (4×2) overlayer. d) STM images showing the individual conformers (A and B) for both the *S* and *R* enantiomers, the associated adsorption footprint is indicated. Thus, the mirroring protrusions of conformer A relate to molecules of opposing chirality. The same is also true for conformer B. In addition, conformer A of the *R* enantiomer has the same adsorption footprint as conformer B of the *S* enantiomer and vice versa (red = *S* enantiomer, blue = *R* enantiomer, filled triangle = conformer A, open triangle = conformer B).

STM images provide information on both molecular chirality and the adsorption-footprint chirality.

STM images of (*R*,*S*)-proline on Cu(110) at 300 K (Figure 2a) reveal an arrangement similar to the (4×2) enantiopure overlayer.[12] Images also show "bright" and "faint" molecules indicating the presence of both conformers A and B identified in the enantiopure system.[12] In contrast to the regular (4×2) pattern of the enantiopure layer, the distribution of conformers in the racemic overlayer is random, Figure 2a, leading to a "pseudo" (4×2) adlayer. High-resolution STM images (Figure 2b,c) enable more detailed information to be extracted. First, conformer B images with a distinct triangular shape, which lies in one of two mirror directions with respect to the [1$\bar{1}$0] axis (Figure 2b). Second, at high image contrast, conformer A images as a tilted oval, in mirrored orientations, indicated in Figure 2c. By comparison with the enantiopure systems we attribute the mirroring protrusions of conformer A and of conformer B to molecules of opposing chirality (Figure 1d). Additionally, regardless of molecular conformation, all protrusions oriented in the same direction possess the same adsorption footprint as shown in Figure 1d. Thus, both the molecular and footprint chirality can be identified at the single-molecule level within the racemic amino acid assembly.

For molecules within a row along the [001] axis, a random mixture of conformers A (bright) and B (faint) is present, with all the protrusions oriented in the same direction, corresponding to a random distribution of enantiomers but all having the same adsorption footprint. For adjacent rows above and below, the protrusions are oriented in the opposite direction (Figure 2b), adopting the mirror adsorption footprint. Thus, the adsorption footprints adhere strictly to a specific heterochiral pattern (Figure 2d) and the arrangement is dictated by the chirality of the adsorption footprint, and not that of the molecule. Essentially, the enantiomers adopt the conformation that allows the adsorption-footprint chirality to be maintained along the row (Figure 2d).

Each molecular row consists of a random sequence of molecular chiral motifs and is, effectively, a diastereoisomer.[20] Thus, the creation of random 2D solid solutions can be induced simply by surface interactions without introducing perturbations, such as enantiospecific substitutions[21] or chiral biases.[22] Such randomizations of enantiomer arrangements are important steps towards yielding non-racemic libraries of oligomers in subsequent polymerization processes[23] and have potential implications for the origin of the homochirality of life.[17]

To gain further insight, periodic DFT calculations were undertaken. Models for a racemic (4×2) overlayer were constructed using conformers A and B (Figure 3a,e) separately, with a heterochiral adsorption-footprint arrangement derived from experiment (Figure 3b,f). Adsorption energies for the overlayers shown in Figure 3a,e were calculated at 1.40 and 1.36 eV/molecule, respectively. The adsorption energy calculated for the enantiopure system in the same footprint arrangement was 1.38 eV/molecule,[12] showing there is no energy penalty for accommodating molecules of opposing chirality into the heterochiral footprint template. Simulated STM images for both conformer A and B racemic models (Figure 3c,g) offer excellent agreement with experiments (Figure 3d,h).

To model the mixed-conformer, mixed-enantiomer overlayer (Figure 4a,b) we investigated the energetics of creating "defects" within a (4×2) layer of conformer B (Figure 3e,f) by substituting in a molecule of conformer A. There are four ways of creating this defect, depending on the molecular chirality and footprint of the defect molecule (defects I–IV, Figure 4c–f, respectively). The relative energies, with respect to the structure in Figure 3e, of defects I–IV were calculated at −0.03, +0.12, +1.22, and +1.35 eV, respectively. STM images were simulated for each defect arrangement for comparison with experiment, Figure 4g–j, respectively. In contrast to defects I and II, both defects III and IV have

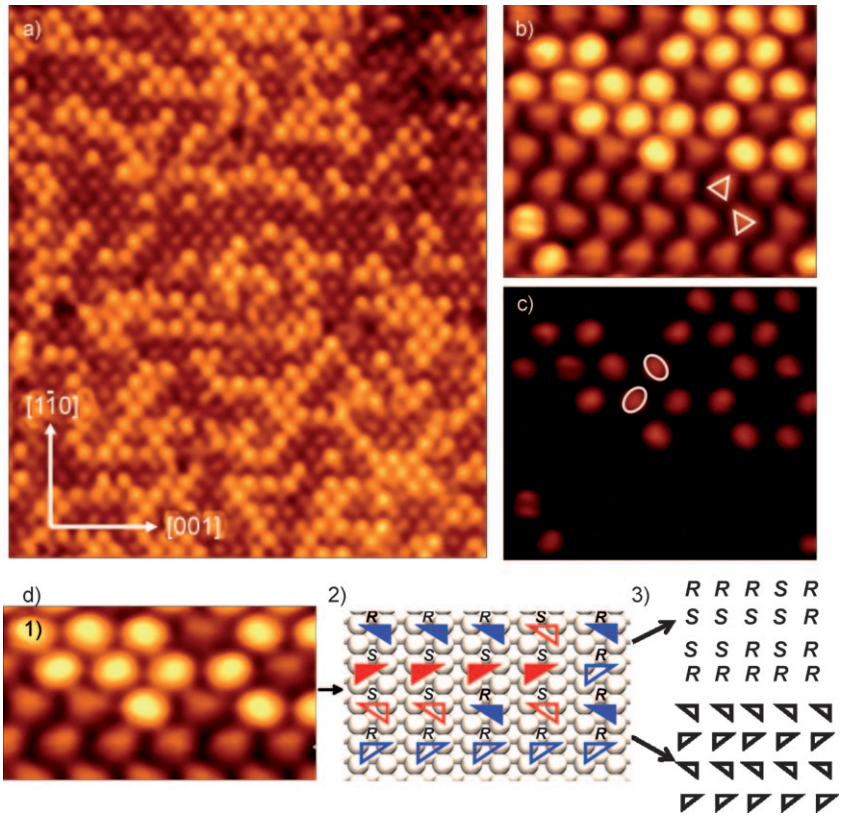

Figure 2. a) STM image of the (*R*,*S*)-proline overlayer on Cu(110) (158×125 Å^2, $I(t) = -0.62$ nA, $V(t) = -1238$ mV). b) and c) High-resolution images showing mixed-conformer, mixed-chirality overlayer (44×50 Å^2, $I(t) = -0.49$ nA, $V(t) = -856$ mV) at differing image contrast. d) 1) Enlarged STM image from (b) (37×43 Å^2), 2) the chirality and the adsorption footprint of each molecule is indicated (key for footprints and chirality as in Figure 1), 3) deconstruction of the image into its molecular chirality and adsorption-footprint arrangement.

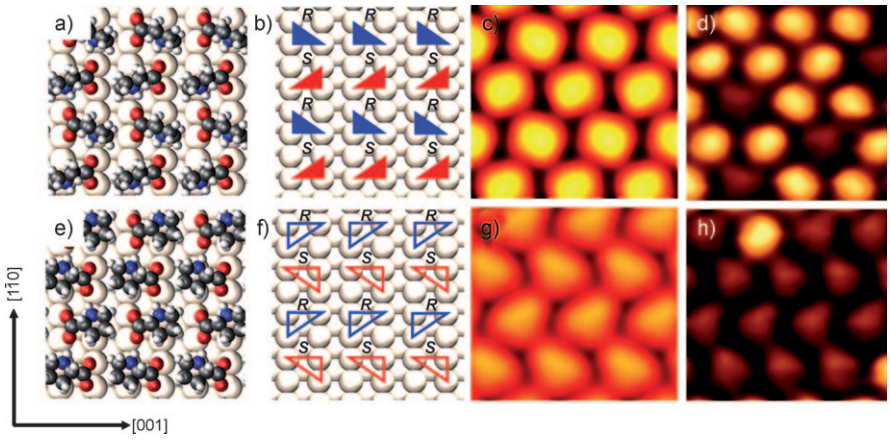

Figure 3. Conformer A: a) DFT optimized model for a (4×2) unit containing mixed enantiomers (color scheme as in Figure 1). b) Diagram representing the molecular adsorption-footprint arrangement (red triangles = *R* enantiomer, blue = *S* enantiomer). c) STM simulation for the model shown in (a) defined as a plot of the constant integrated local density of states, at an energy of −0.89 eV (16.6×21.5 Å^2). d) STM image showing cluster of racemic molecules of conformer A (25×25 Å^2, $I(t) = -0.49$ nA, $V(t) = -856$ mV). e)–h) The corresponding information for conformer B (STM image conditions, 26×23 Å^2, $I(t) = -0.49$ nA, $V(t) = -856$ mV).

highly unfavorable energetics and the agreement between simulated images and experiment is poor, thus defects III and IV can be discounted. Defect I has a more favorable relative energy than defect II and is the only defect that follows the experimentally observed heterochiral footprint arrangement. The negligible relative energy of defect I confirms that the footprint arrangements, not the molecular chirality, determine organization. This result is reinforced by the STM image, Figure 4b, of an alternative defect where conformer B is accommodated within a conformer A hexagon.

Several chemical forces drive the specific heterochiral footprint arrangement adopted in the racemic system. A large destabilization for defects III and IV arises from repulsive interactions and a compressive strain induced by a local increase in the Cu–Cu spacing,[24] which occurs when adjacent carboxylate groups are bonded to neighboring Cu atoms in the [1$\bar{1}$0] row. Thus, only those adsorption-footprint arrangements that avoid such juxtapositions are preferred (e.g. the enantiopure layer (Figure 1c) the racemic conformer A and B structures (Figure 3b,f) and defects I and II). In addition, defects I and II are stabilized by the formation of hydrogen bonds, with the hydrogen atom of the amino group interacting with the oxygen atom of the carboxylate group to form a strong hydrogen bond.[12] Hydrogen-bonding interactions for the racemic A and B conformer structures (Figure 3a,e), and each defect structure are summarized in Figure 5. The racemic A and B conformer structures (Figure 5a,b) and the defect I structure (Figure 5c) all maintain the strong hydrogen-bonded chains in the [1$\bar{1}$0] direction. Thus, within the specific heterochiral-footprint arrangement, conformer A of (*R*)-proline is equivalent to the B conformer of (*S*)-proline, with respect to the formation of hydrogen-bonded chains. Defect II has the same number of strong hydrogen bonds, but unfavorable steric interactions between neighboring CH_2 group are incurred. Therefore, we suggest that the stability of the specific heterochiral-footprint template adopted is also due to its ability to sustain hydrogen-bonded chains. We note previous calculations by Rankin and Sholl[11] also predicted a

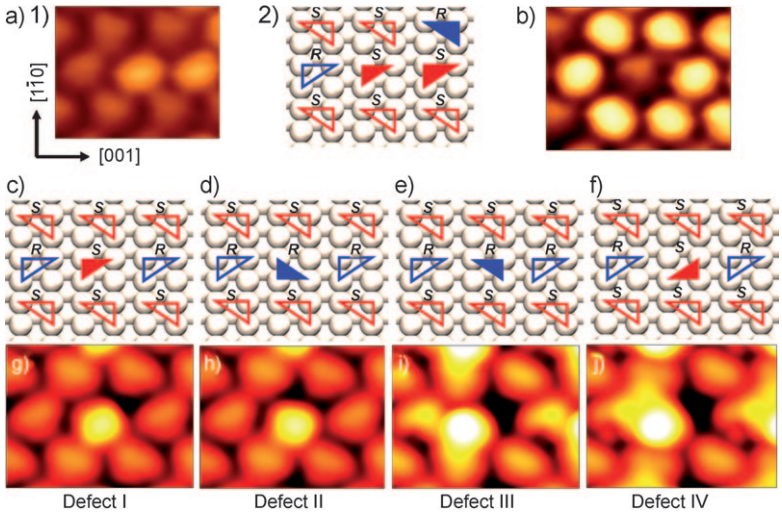

Figure 4. a) 1) STM image showing a "defect" (4×2) unit (16.3×21.6 Å^2, $I_t = -0.42$ nA, $V_t = -1250$ mV). 2) Schematic representation of the adsorption-footprint arrangement as determined from experiment. b) STM image of the alternative "mirror" defect to that shown in (a) (15.7×23.4 Å^2, $I_t = -0.49$ nA, $V_t = -806$ mV). c–f) Schematic diagrams representing the adsorption-footprint arrangements of defects I–IV, respectively (code for molecular and footprint chirality as in Figure 1c). g–j) Calculated STM simulations for defects I–IV, respectively.

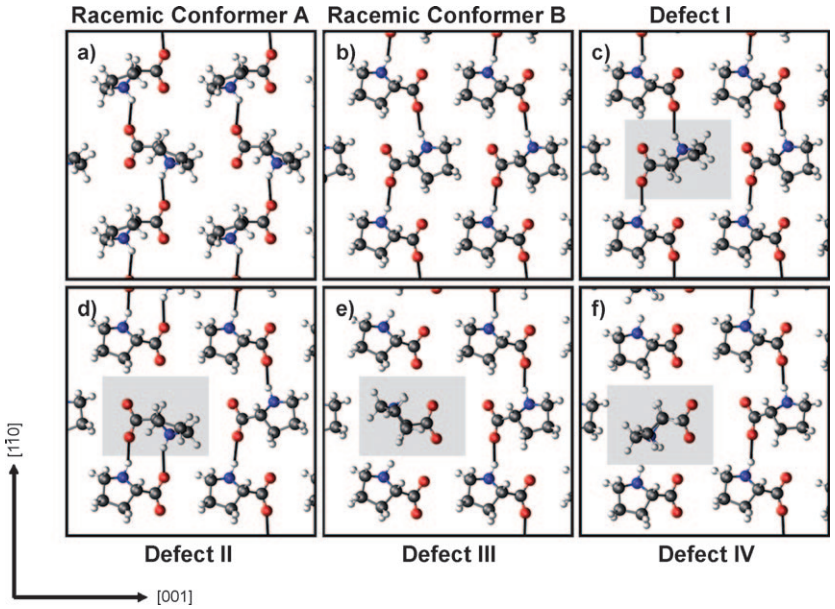

Figure 5. Hydrogen-bonding arrangement for a) racemic conformer A (4×2) unit, b) racemic conformer B (4×2) unit, c) defect structure I, d) defect structure II, e) defect structure III, f) defect structure IV. Color code is as in Figure 1. Strong hydrogen bonds are indicated by solid black lines, shaded boxes in (c–f) indicate a defect molecule. A strong hydrogen bond is defined in this case as the interaction between hydrogen and oxygen at a distance of less than 2.2 Å. Diagrams showing all hydrogen bonding interactions in the models shown may be found in the Supporting Information, Figures S1 and S2.

heterochiral-footprint organization with a random dispersion of molecular chirality in the (3×2) structure of (*R*,*S*)-alanine on Cu(110); however, no experimental verification existed owing to an inability to distinguish either molecular or footprint chirality by STM.[10]

In conclusion, we have shown from a combined STM and DFT study that the complex racemic prolate (4×2) overlayer can be fully characterized by identification of the adsorption footprint and molecular chirality of each molecule. The organization is found to be solely driven by a strict heterochiral adsorption-footprint template, which minimizes repulsive interactions and maximizes hydrogen bonding, and not by the molecular chirality. Thus, each adsorption position in the template can be occupied by either enantiomer resulting in a 2D random solid solution at the surface. Given that amino acids crystallize in 3D as racemic compounds, this result highlights that, compared to 3D, there are greater opportunities at surfaces for creating random solid solutions, induced by adsorption effects. This work also suggests that targeted modifications that influence adsorption footprints at surfaces are a vital step towards controlling chiral organization in molecular monolayers.

Experimental Section

STM data was collected in a Specs Aarhus 150 STM operated in constant current mode. Experiments were conducted in ultra-high vacuum chambers ($P < 2\times10^{-10}$ mbar). (*R*,*S*)-proline (99%, Sigma Aldrich) was sublimed onto clean Cu(110) at room temperature. The (4×2) overlayer was established by LEED and the presence of the prolate species confirmed by RAIRS.[12] Periodic density functional theory calculations were preformed using the VASP code[25] and simulated STM images calculated using the Tersoff–Hamann approximation[26] as described elsewhere.[12]

Received: September 4, 2009
Revised: November 17, 2009
Published online: February 28, 2010

Keywords: amino acids · chirality · scanning probe microscopy · solid solutions · surface chemistry

[1] L. Pasteur, *Ann. Phys.* **1848**, *24*, 442.
[2] J. Jacques, A. Collet, S. H. Wilen, *Enantiomers, Racemates and Resolutions*, Kreiger Publishing Company, Malabar, FL, **1994**; L. Perez-Garcia, D. B. Amabilino, *Chem. Soc. Rev.* **2002**, *31*, 342; L. Perez Garcia, D. Amabilino, *Chem. Soc. Rev.* **2007**, *36*, 941.
[3] I. Kuzmenko, I. Weissbuch, E. Gurovich, L. Leiserowitz, M. Lahav, *Chirality* **1998**, *10*, 415.
[4] M. Ortega Lorenzo, C. J. Baddeley, C. Muryn, R. Raval, *Nature* **2000**, *404*, 376; J. A. A. W. Elemans, I. De Cat, H. Xu, S. De Feyter, *Chem. Soc. Rev.* **2009**, *38*, 722; R. Raval, *Chem.*

Soc. Rev. **2009**, *38*, 707; M. Parschau, D. Passerone, K.-H. Rieder, H. J. Hug, K.-H. Ernst, *Angew. Chem.* **2009**, *121*, 4125; *Angew. Chem. Int. Ed.* **2009**, *48*, 4065; T. Huang, Z. Hu, A. Zhao, H. Wang, B. Wang, J. Yang, J. G. Hou, *J. Am. Chem. Soc.* **2007**, *129*, 3857; M. C. Blüm, E. Cavar, M. Pivetta, F. Patthey, W.-D. Schneider, *Angew. Chem.* **2005**, *117*, 5468; *Angew. Chem. Int. Ed.* **2005**, *44*, 5334; S. Stepanow, N. Lin, F. Vidal, A. Landa, M. Ruben, J. V. Barth, K. Kern, *Nano Lett.* **2005**, *5*, 901; Y. Cai, S. L. Bernasek, *J. Phys. Chem. B* **2005**, *109*, 4514.

[5] E. Mateo Marti, S. M. Barlow, S. Haq, R. Raval, *Surf. Sci.* **2002**, *501*, 191; M. Lingenfelder, G. Tomba, G. Costantini, L. C. Ciacchi, A. De Vita, K. Kern, *Angew. Chem.* **2007**, *119*, 4576; *Angew. Chem. Int. Ed.* **2007**, *46*, 4492; A. Kühnle, T. R. Linderoth, F. Besenbacher, *J. Am. Chem. Soc.* **2003**, *125*, 14680; A. Kuhnle, T. R. Linderoth, B. Hammer, F. Besenbacher, *Nature* **2002**, *415*, 891; A. Schiffrin, A. Riemann, W. Auwarter, Y. Pannec, A. Weber-Bargioni, D. Cvetko, A. Cossaro, A. Morgante, J. V. Barth, *Proc. Natl. Acad. Sci. USA* **2007**, *104*, 5279; X. Zhao, H. Yan, R. G. Zhao, W. S. Yang, *Langmuir* **2003**, *19*, 809; V. Humblot, C. Mthivier, C. M. Pradier, *Langmuir* **2006**, *22*, 3089; X. Zhao, Z. Gai, R. G. Zhao, W. S. Yang, T. Sakurai, *Surf. Sci.* **1999**, *424*, L347; X. Zhao, R. G. Zhao, W. S. Yang, *Surf. Sci.* **1999**, *442*, L995; H. Iwai, M. Tobisawa, A. Emori, C. Egawa, *Surf. Sci.* **2005**, *574*, 214; T. E. Jones, C. J. Baddeley, A. Gerbi, L. Savio, M. Rocca, L. Vattuone, *Langmuir* **2005**, *21*, 9468; V. Feyer, O. Plekan, T. Skala, V. Chab, V. Matolin, K. Prince, *J. Phys. Chem. B* **2008**, *112*, 13655.

[6] S. M. Barlow, K. J. Kitching, S. Haq, N. V. Richardson, *Surf. Sci.* **1998**, *401*, 322; N. A. Booth, D. P. Woodruff, O. Schaff, T. Giessel, R. Lindsay, P. Baumgartel, A. M. Bradshaw, *Surf. Sci.* **1998**, *397*, 258; J.-H. Kang, R. L. Toomes, M. Polcik, M. Kittel, J.-T. Hoeft, V. Efstathiou, D. P. Woodruff, A. M. Bradshaw, *J. Chem. Phys.* **2003**, *118*, 6059.

[7] R. B. Rankin, D. S. Sholl, *J. Phys. Chem. B* **2005**, *109*, 16764.

[8] M. Nyberg, M. Odelius, A. Nilsson, L. G. M. Pettersson, *J. Chem. Phys.* **2003**, *119*, 12577; S. Blankenburg, W. G. Schmidt, *Nanotechnology* **2007**, *18*, 424030.

[9] S. M. Barlow, S. Louafi, D. Le Roux, J. Williams, C. Muryn, S. Haq, R. Raval, *Surf. Sci.* **2005**, *590*, 243; G. Jones, L. B. Jones, F. Thibault-Starzyk, E. A. Seddon, R. Raval, S. J. Jenkins, G. Held, *Surf. Sci.* **2006**, *600*, 1924; D. I. Sayago, M. Polcik, G. Nisbet, C. L. A. Lamont, D. P. Woodruff, *Surf. Sci.* **2005**, *590*, 76; J. Williams, S. Haq, R. Raval, *Surf. Sci.* **1996**, *368*, 303.

[10] S. Haq, A. Massey, N. Moslemzadeh, A. Robin, S. M. Barlow, R. Raval, *Langmuir* **2007**, *23*, 10694.

[11] R. B. Rankin, D. S. Sholl, *Surf. Sci.* **2004**, *548*, 301; J. N. James, D. S. Sholl, *Curr. Opin. Colloid Interface Sci.* **2008**, *13*, 60.

[12] M. Forster, M. S. Dyer, M. Persson, R. Raval, *J. Am. Chem. Soc.* **2009**, *131*, 10173.

[13] N. L. Rosi, C. A. Mirkin, *Chem. Rev.* **2005**, *105*, 1547; Y. W. C. Cao, R. Jin, C. A. Mirkin, *Science* **2002**, *297*, 1536.

[14] Y. Izumi, *Adv. Catal.* **1983**, *32*, 215.

[15] C. Joachim, J. K. Gimzewski, A. Aviram, *Nature* **2000**, *408*, 541; R. J. Heath, P. J. Keukes, G. S. Snider, R. S. Williams, *Science* **1998**, *280*, 1716; L. A. Bumm, J. J. Arnold, M. T. Cygan, T. D. Dunbar, T. P. Burgin, L. Jones II, D. L. Allara, M. J. Tour, P. S. Weiss, *Science* **1996**, *271*, 1705; L. Romaner, G. Heimel, M. Gruber, J.-L. Bredas, E. Zojer, *Small* **2006**, *2*, 1468.

[16] R. M. Kellogg, B. Kaptein, T. R. Vries, *Top. Curr. Chem.* **2007**, *269*, 159; G. Coquerel, *Top. Curr. Chem.* **2007**, *269*, 1.

[17] M. Avalos, R. Babiano, P. Cintas, J. L. Jimenez, J. C. Palacios, *Origin Life Evol. Biosph.* **2004**, *34*, 391; J. S. Siegel, *Chirality* **1998**, *10*, 24; W. A. Bonner, *Origin Life Evol. Biosph.* **1994**, *24*, 63; I. Weissbuch, G. Bolbach, L. Leiserowitz, M. Lahav, *Origin Life Evol. Biosph.* **2004**, *34*, 79.

[18] S. M. Barlow, R. Raval, *Surf. Sci. Rep.* **2003**, *50*, 201.

[19] C. Vidma, *Origin Life Evol. Biosph.* **2001**, *31*, 501.

[20] Diastereoisomers are stereoisomers that are not mirror images of each other. If the sequence of molecules along the [001] axis consisted of alternate rows of *SSSS* and *RRRR* then the chains would be truly enantiomeric. However, the random nature of the distribution of chiral motifs along the [001] axis generates sequences that are not mirror images, for example, *RSRS* and *SSRR*, which are diastereoisomers.

[21] N. Liu, S. Haq, G. R. Darling, R. Raval, *Angew. Chem.* **2007**, *119*, 7757; *Angew. Chem. Int. Ed.* **2007**, *46*, 7613.

[22] S. Haq, N. Liu, V. Humblot, A. P. J. Jansen, R. Raval, *Nat. Chem.* **2009**, *1*, 409; I. Weissbuch, L. Leiserowitz, M. Lahav, *Top. Curr. Chem.* **2005**, *259*, 123; R. Fasel, M. Parschau, K. H. Ernst, *Nature* **2006**, *439*, 449; M. Parschau, S. Romer, K. H. Ernst, *J. Am. Chem. Soc.* **2004**, *126*, 15398.

[23] J. P. Ferris, A. R. Hill, R. Liu, L. E. Orgel, *Nature* **1996**, *381*, 59; R. M. Hazen, T. R. Filley, G. A. Goodfriend, *Proc. Natl. Acad. Sci. USA* **2001**, *98*, 5487.

[24] C. G. M. Hermse, A. P. Van Bavel, A. P. J. Jansen, L. A. M. M. Barbosa, P. Sautet, R. A. Van Santen, *J. Phys. Chem. B* **2004**, *108*, 11035.

[25] G. Kresse, J. Furthmüller, *Phys. Rev. B* **1996**, *54*, 11169.

[26] J. Tersoff, D. R. Hamann, *Phys. Rev. Lett.* **1983**, *50*, 1998.

